

PAPER • OPEN ACCESS

Energy Optimal Intelligent Switching Mechanism for Induction Motors with Time Varying Load

Recent citations

- [R. Rajesh Kanna et al](#)

To cite this article: R. Raja Singh *et al* 2020 *IOP Conf. Ser.: Mater. Sci. Eng.* **906** 012017

View the [article online](#) for updates and enhancements.



ECS **240th ECS Meeting**
Oct 10-14, 2021, Orlando, Florida

Register early and save up to 20% on registration costs

Early registration deadline Sep 13

REGISTER NOW

Energy Optimal Intelligent Switching Mechanism for Induction Motors with Time Varying Load

R. Raja Singh¹, C. Thanga Raj², Ryszard Palka³, V. Indragandhi¹, Marcin Wardach³, and Piotr Paplicki³

¹ Advanced Drives Laboratory, Department of Energy and Power Electronics, Vellore Institute of Technology, India.

² Hydropower Simulation Laboratory, Department of Water Resources Development & Management, Indian Institute of Technology Roorkee, India.

³ Department of Power Systems and Electrical Drives West Pomeranian University of Technology in Szczecin, Poland.

Correspondence: rrajasingh@gmail.com

Abstract. In medium and small process industries Induction Motor (IMs) enabled star-delta energy conservation scheme is a common practice. In such industrial applications, the Power Quality Disturbances (PQD) must be considered for hassle free operation. This paper is an attempt in the above direction on star-delta energy conservation applied to IMS (2.2 kW and 37.5 kW) operated with time varying loads. In apart to machine's performance evaluation, variation of switchover point for uninterrupted operation and optimized energy savings under various electrical perturbations is realized. Moreover, safe restarting feature is equipped in controller for resuming the machine during unplanned shutdown or any interruption.

Keywords: energy conservation; power quality disturbances; star-delta scheme; switchover point; squirrel cage induction motor

1. Introduction

Energy conservation (EC) is a key requirement for any industry, and most industries are following it economically. Processing industries, textile mills, tiles mills, paper mills, leather mills, etc., generally prefer IMs because of their reliability and robustness, but these engines run out inefficiently during part load operation. Electrical machines are designed and around the full load to achieve maximum output and high power factor. Therefore, the part-load system results in inefficiency and inadequate power factor [1]. The electrical grid with many partially charged motors, causes inadequate power factor and causes instability of voltage. Optimally, the efficiency and the power factor of the motor will be improved. Therefore, an energy-optimal strategy is mandatory for all industries without affecting machine performance. Although there are plenty of energy conservation techniques available, due to investment constraints, most industrialists show less interest in adopting energy-efficient technologies. In this field, several researchers are developing various economy energy conservation scheme that receive considerable attention [3]. Kothals Altes et al. initially introduced the induction motor star delta scheme for decreasing magnetizing current [4]. The energy-saving aspect of the scheme was later attempted by Alger et al. with a harmonic distortion analysis [5]. Taylor, et al. achieves optimum load-based motor torque demand by automatic star-delta configuration [6]. Gjota et al. modified engine windings to improve IM performance [7]. Ferreira, and so on. Miloje, et al. predicted a power factor enhancement star delta energy conversion scheme using PIC microcontroller [8–9]. In another path, through the adoption of drive technology, different energy conservation schemes are implemented. Advancing control techniques and electronic power topologies has energy-efficient operation on industrial drives, but these electronic power controls are very expensive. In addition, electronic power switches could be the origin of harmonics, leading to device instability and girding [10]. In addition, the overall power electronic drive system efficiency is reduced due to losses in switching and conduction [11]. Through controlling the flux using various control techniques the efficiency of the IMs is



accomplished with energy conservation [12–16]. The issues regarding energy saving (e.g. through increased efficiency) have also been discussed in papers related to other types of machines, e.g. linear induction machines [17] or hybrid excited machines [18–19].

On the other hand, these electrical drives in any industry are influenced by various electrical perturbations, and causes process interruptions and equipment failure [20]. Severity of PQD in star-delta scheme based EC is more as motor windings receive less voltage at star mode. This paper, therefore, analyses the star-delta energy conservation system in IM under different PQDs including under-voltage, over-voltage, voltage sag, voltage unbalance, under-frequency, over-frequency, and single phasing. Considering these PQDs, a strategic approach for continuous operation is provided through automatically readjusting the switch over point. Moreover, safe restarting feature is embedded in the proposed controller for resuming the machine during unplanned shutdown or any interruption. (i.e.) Conventional star-delta energy saving scheme resume only in star connection, however, star connected motor fails to develop sufficient torque at heavy loads. Focusing on this direction, the last operating mode is recorded for safe restarting in the proposed strategy. A 37.5 kW induction motor spinning machine of a medium scale textile industry is considered as a case study. The motivation of this work is to enforce the proposed controller for providing reliable energy conservation in small and medium scale process industries where conventional star-delta starter is employed.

In overall, the paper contains the description of experimental arrangement in section 2, besides, a case study with star delta based energy conservation has been carried out using the load curve of textile spinning mill in section 3. Effect of power quality disturbances on Y- Δ scheme based IM in section 4, summary of PQD with an intelligent switching mechanism in section 5 and concluded in section 6.

2. Experimentation

Laboratory tests are carried out on the basis of theory and empirical evidence to discover the effects of the proposed energy saving strategy and to analyze the test machine's behavior. Systematic operation is performed to obtain the results for analysis.

2.1. Experimental Arrangement

Dynamic performance of a 2.2 kW IM is analyzed experimentally and a 37.5 kW IM is simulated using Matlab/Simulink software. Experimental arrangement (Fig. 1) consists of a 2.2 kW squirrel cage induction motor (SCIM) coupled with dynamometer loading arrangement (DC generator, excitation system, and electrical load). Machine parameters are given in Table 1. An AC programmable power supply (AMETEK 3000 Lx) is used to inject various electrical disturbances on test machine and the electrical quantities are measured recorded using three-phase power quality analyzer (PQA – Fluke 435).

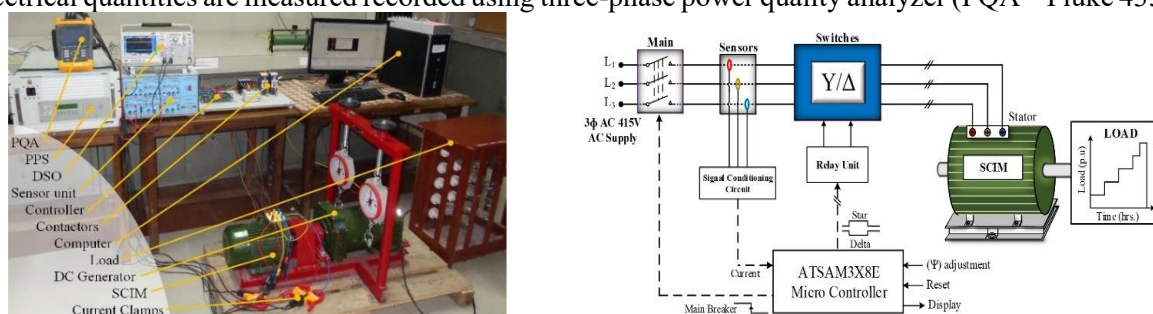


Figure 1. Experimental arrangement for Y- Δ Scheme (a) Experimental Arrangement (b) Schematic diagram of Y- Δ Scheme.

Similarly, the output quantities (speed, torque, and temperature) are measured using tachogenerator, electro dynamo meter arrangement and thermal imager (FLUKE Ti-32) respectively. The control strategy consists of sensor unit (Hall Effect current and voltage sensors) with signal conditioning circuit to provide the digital signals to controller. Atmel micro-controller (ATSAM3X8E) with opto-coupler

isolated driver and relay unit is used to drive the contactors with respect to load variation. Two contactors are used for switching the winding connections alternatively (star or delta), additionally a main contractor is used to energize or isolate the system from supply voltages.

Table 1. Machine particulars.

| Particulars | Induction Machine | DC Machine |
|-----------------|-------------------|-------------|
| Rated Power | 2.2 kW | 2.2 kW |
| Rated Voltage | 415 V | 220 V |
| Rated Current | 4.7 A | 12 A |
| Rated Frequency | 50 Hz | – |
| Rated Speed | 1410 rpm | 1500 rpm |
| No. of poles | 4 poles | 4 poles |
| Type | Squirrel Cage | Shunt |
| Cooling Type | Fan cooling | Fan cooling |

2.2. Experimental Arrangement

As per IEEE 112TM-2004 benchmark [21], an experiment is performed with the 2.2 kW SCIM (test machine). A load-test is conducted on the test machine with star and delta contact to obtain preliminary results. Using the typical equations (1) to (5) in the collected experimental data, the energy and efficiency load curves are plotted, shown in Fig. 2. Efficiency, energy saving and power factor of the star connected motor is found to be higher than the delta connection during the light load operation, but otherwise during the high load operation. The machine operating with star at light load region is considered as Mode-I and running with the delta at high load region is considered as Mode-II, which enhances the energy-saving and strengthen the machine's performance. Matlab/Simulink software is used to validate the proposed scheme and also for generalizing to the higher machine ratings. Efficiency-load and energy-load profile intersecting point of the star and delta curve is considered to be a switch-over point denoted by Ψ . concerning the machine rating and its parameters, the switchover point varies.

$$\text{Efficiency [\%]} = \frac{P_o}{P_i} \cdot 100 \quad (1)$$

$$\text{Mechanical output power } (P_o) = \omega \cdot T \quad (2)$$

$$\text{Electrical input power } (P_i) = \sqrt{3}U_L I_L \cos \varphi \quad (3)$$

$$\text{Energy} = P_i \cdot \text{time period} \quad (4)$$

$$\text{Power Factor } (\cos \varphi) = \frac{P_i}{S_i} \cdot 100 \quad (5)$$

where, ω is speed of the machine in rad/s, V_L is the input line voltage in volts, T is the output load torque in newton meter, I_L is the input line current in amps and S_i is the apparent power in volt ampere.

This paper's primary objective is to testify the tangible benefits of the Y- Δ energy conservation technique in test machine with minimal capital expenditure, less downtime and resource requirement. Implementation of the Y- Δ energy conservation technique under part-load operations indicates that the power factor, energy-saving, and efficiency are improved significantly. The test machine is operated with a linear step load (Fig. 5b) using conventional and proposed energy saving strategy. All the input electrical quantities including the machine's speed are shown in Fig. 3 and Fig. 4.

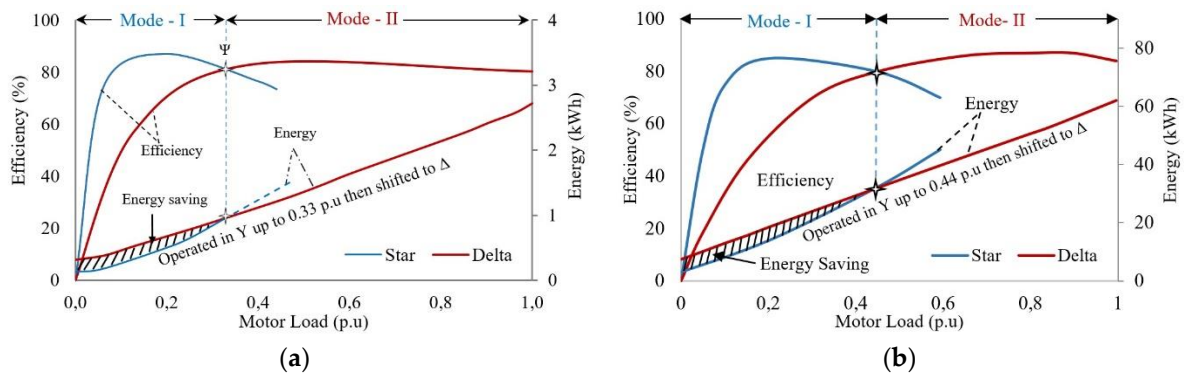


Figure 2. Efficiency and energy profile of star and delta connected SCIM; (a) 2.2 kW IM, (b) 37.5 kW IM.

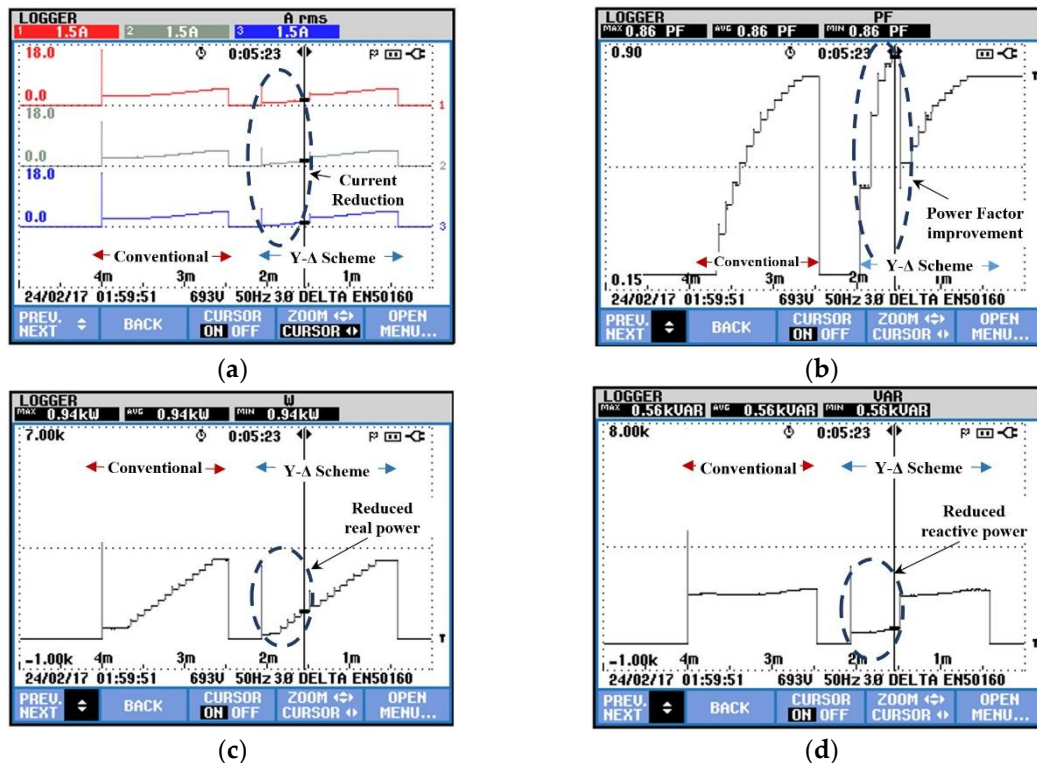


Figure 3. Electrical parameters of SCIM with conventional Δ connected and Y- Δ EC strategy: (a) Input Current; (b) Input Power factor; (c) Input Real power; (d) Input Reactive Power.

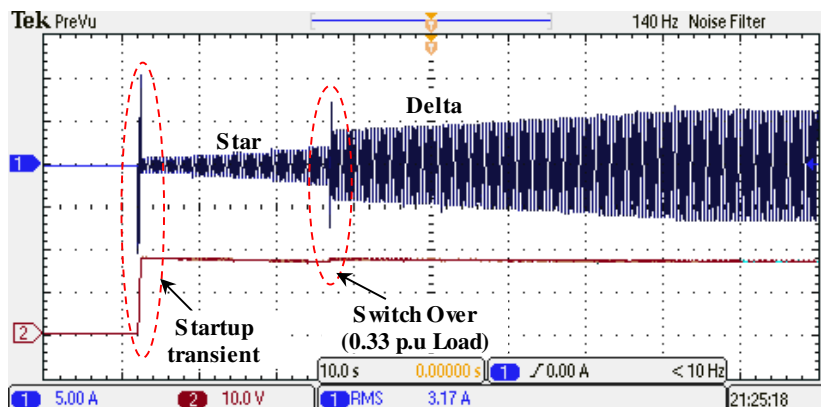


Figure 4. Current and Speed of SCIM with Y- Δ EC strategy process.

Analysis findings are as follows:

2.2.1. Current

Starting the machine with the star connection, provides lesser current transient 33.47 percent lower than direct on-line starting. In addition, the switch-over transient is lower than the starting transient (1.32 p.u.) shown in Fig 3a and Fig 4.

2.2.2. Power factor

At light loads, the machine's power factor with the proposed strategy is greater than the conventional method. The no-load power factor is 43.37 percent higher in the proposed scheme shown in Fig. 3b

2.2.3. Real power

Compared to the conventional method shown in Fig. 3c, the proposed technique conserves 3.68 % more energy, ultimately leading to improved efficiency. Also, it is noted that the amount of energy-saving varies in accordance with the rating of the machine.

2.2.4. Reactive power

Adopting the proposed strategy, the consumption of reactive power is significantly minimized. Operating the machine for a complete cycle (i.e.) no load to full load, the consumption of reactive power in the proposed star-delta scheme is 21.82 percent lesser than the conventional direct scheme is depicted in Fig. 3d. Excess reactive power demand, which is accountable for iron losses, winding losses, and inappropriate loading of the machine.

2.2.5. Speed

At switchover point (0.33 p.u load), the speed of the star-connected system is 4.67 percent lower than the delta-connected system. Nevertheless, it is 0.52 percent higher than the rated speed of the test machine (146.53 rad/sec).

3. Case study on textile spinning mill with star-delta energy conservation strategy

A spinning drive motor in the textile mill is accounted for energy conservation studies. The textile industry has different processes such as spinning, carding, combing and so on, amongst these process, the spinning drive motor consumes more than 50% of total energy [1]. Mechanically acquiring thread from cotton fibers is called the process of spinning, shown in Fig. 5a. The thread quantity on the spindle increases gradually from zero to the total permissible limit during this spinning process (from hollow bobbin to full bobbin), and therefore the load on the spinning drive motor increase to rated value from no-load value, depicted in Fig. 5b. Acquiring the Y- Δ energy conservation strategy in the system of

spinning, the drive motor operates at light load region with star connection and at high load region with delta connection.

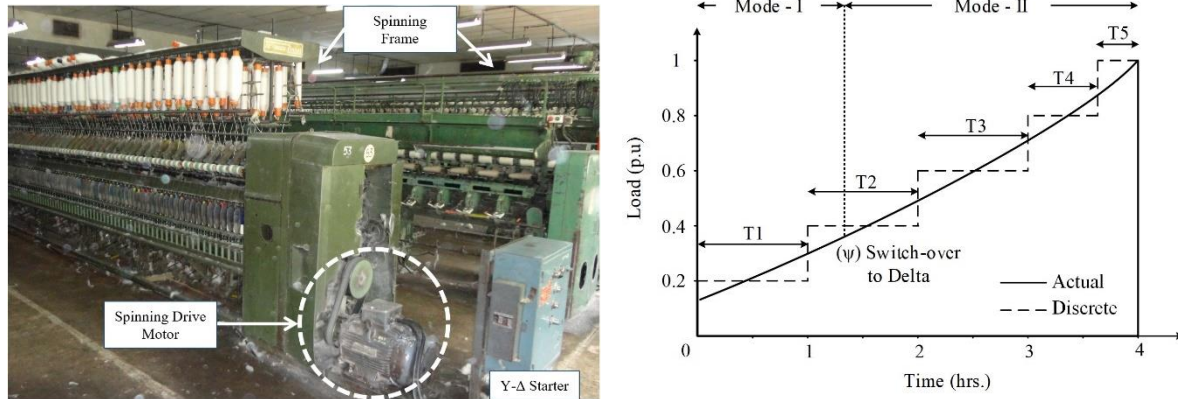


Figure 5. Textile spinning frame with the load diagram: (a) Spinning frame with drive motor; (b) Load diagram of spinning drive motor.

Considering the spinning frame process cycle in the textile mill (360 workdays per year with 5 processes cycle per day and 4 hrs per cycle process), annual energy saving is calculated using equation 6 and shown in Table 2. From the results, it is observed that Y-Δ scheme offers 3.68 % and 5.97 % of energy conservation in 2.2 kW and 37.5 kW IM, respectively. In addition, under the star-delta scheme, IM ensures better power factor improvement and thermal effect reduction.

$$E_s = (E_{c\Delta} - E_{cY}) * H_T \tag{6}$$

$$E_{c\Delta} = \sum_{n=1}^{\infty} \left\{ \frac{(x_{n+1} - x_n)(y_{\Delta n+1} + y_{\Delta n})}{2} \right\} \tag{7}$$

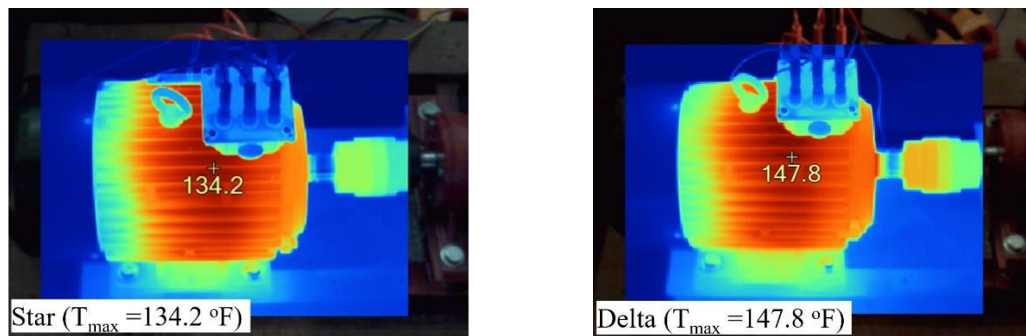
$$E_{cY} = \sum_{n=1}^{\infty} \left\{ \frac{(x_{n+1} - x_n)(y_{Y n+1} + y_{Y n})}{2} \right\} \tag{8}$$

Where, E_s is the total energy saved in kWh, $E_{c\Delta}$ is energy consumed per process with conventional delta (Δ) connection in kWh, E_{cY} is total energy consumed per process using star-delta (Y- Δ) scheme in kWh, H_T is total working hours per annum, n is number of samples, x is process time in hours, y_{Δ} is power consumed with conventional delta connection in kW, y_Y is power consumed using star-delta scheme in kW.

Moreover, the temperature of test machine is measured for analyzing the thermal effect at light load with star and delta winding connections. Since the proposed system is mainly meant for small and medium scale industries, the rating of the machine is lower where fan type cooling is mainly used [IEC 60034-1] and the cooling of motor directly proportional to shaft revolution. Corresponding to load diagram (Fig. 5b), test machine is operated from no load to 0.33 p.u. load in 1.2 hours with star and delta connection individually and snapshot of test results is shown in Fig. 6a and 6b. It is observed that, machine with star connected produces 13.6 °F less temperature than the machine with delta connection. As the temperature produced in machine is proportionate to the voltage and current in windings, SCIM with star connection produces less thermal effect than delta connection. These variances of thermal characteristics are common for other higher capacity machines (37.5 kW)

Table 2. Energy conserved in IM using Y- Δ scheme with machine constants.

| Machine rating | Switchover point (ψ) | Energy Consumed kWh / year | | Energy Saving kWh / year | Total cost saving / year (\$) # |
|---|--|----------------------------|---------------------|--------------------------|---------------------------------|
| | p.u load | Y- Δ Scheme | Normal (Δ) | | |
| 2.2 kW* | 0.33 | 9721 | 10091 | 371 | 39 |
| 37.5 kW** | 0.44 | 231990 | 246739 | 14749 | 1520 |
| Machine constants | | | | | |
| 2.2 kW* | $R_1 = 3.678, R_2 = 1.3, X_1 = X_2 = 7.813, X_m = 88.57$ | | | | |
| 37.5 kW** | $R_1 = 0.0823, R_2 = 0.0503, X_1 = X_2 = 0.2274, X_m = 8.51$ | | | | |
| * Experimentation & Simulation; ** Simulation; # Considered 0.103 \$ per kWh [22]. Considered as class A for empirical distribution of leakage reactance [21] R_1 and X_1 are the resistance and the reactance of the stator in ohms, R_2 and X_2 are the resistance and the reactance of rotor referred to the stator in ohms, X_m is the magnetizing reactance in ohms. | | | | | |

**Figure 6.** Thermal Effect of 2.2 kW IM in light load region (Mode-I): (a) Y- Δ scheme, (b) normal operation (Δ).

4. Electrical perturbations on Y- Δ scheme enabled IM

Most aged industries are concerned about issues of power quality including voltage sag, under-voltage, over-voltage, voltage unbalance, under-frequency, over-frequency, single phasing and harmonics. Such fluctuations in power performance are usually caused by non-linear loads, system failures, direct line starting of motor, imbalance loads, power conversion switching, uneven distribution of single phase loads etc. [20–23]. Power quality disturbances (PQD) have a detrimental effect on the industrial drive motor and the degree of impact on the motor is dependent on its connections and span. Fortunately, the use of power quality analyzers to measure PQD easily as they are longer and slower lasting events [1]. This section analyses the effects of various PQD in Y- Δ schemed IM at light loads and compared the results with conventional delta connected IM. Experimentally, power quality disturbances are created and analyzed using AC programmable power supply (AMETEK 3000Lx) and three phase power quality analyzer (Fluke - 435) respectively. To validate the obtained experimental results and to generalize with higher machine rating, Matlab/Simulink software is used.

4.1. Voltage sag

Voltage sag is defined as the momentary variation in voltage magnitude between 10 and 90 percent of nominal value from half cycle to one minute [24]. Voltage sag is created due to various factors such as short circuit faults, starting of motors in same bus, single line to ground faults, etc., Voltage sag is the most common problem in industries, that reduces the efficiency and life span of machine. Also, sag affects the quality of end product in process industries [25]. During voltage sag, due to small time

constant, the electromagnetic torque reduces in proportional to square of sag depth (rms value) without changing mechanical torque. This reduction of electrical torque force to operate the motor at a new operating point with speed reduction, thereby exerted torque on motor may fail to drive the load [26]. The test machine is experimentally analyzed by allowing it to experience 10 to 60 percent of three phase single event symmetrical voltage sag for 1 sec, shown in Fig. 7. Similarly, 2.2 kW and 37.5 kW SCIM are analyzed using Matlab/Simulink software with the same percentage of voltage sag for generalization.

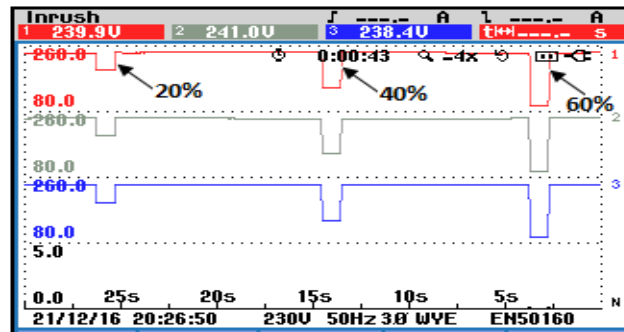


Figure 7. Symmetrical voltage sag (20%, 40% and 60%).

It is observed that, voltage sag induces current transients, but comparatively lesser than the starting and switchover transients. In case of star connected IM, sag creates heavy flow of current (transient) due to magnetic saturation, whereas, the transient is lower in delta connected IM due to absence of magnetic saturation. Similarly, torque of star connected IM gets affected three times more than the delta connected induction motor. Also, the star connected IM experiences more drop in speed than the delta connected motor shown in Fig. 8, which could reduce the quality of the end product and cause heavy loss to industries.

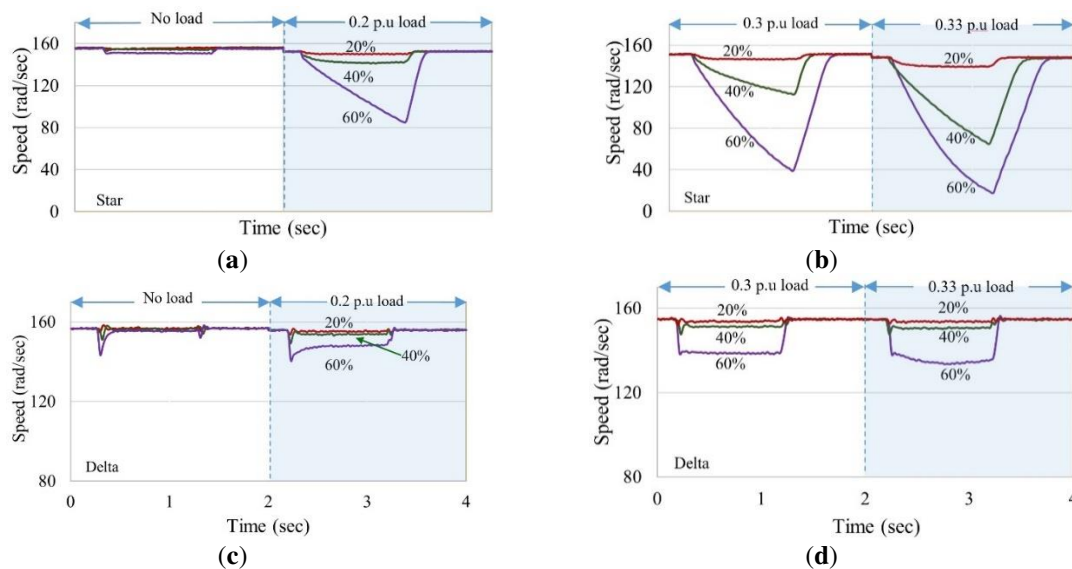


Figure 8. Speed variation of 2.2 kW IM during voltage sag (20%, 40% and 60%): (a) Star at No load and 0.2 p.u. load; (b) Star at 0.3 p.u. and 0.33 p.u. load; (c) Delta at No load and 0.2 p.u. load; (d) Delta at 0.3 p.u. and 0.33 p.u. load.

Assuming if 20 percent of speed variation is allowed in a process industry, 2.2 kW SCIM with Y- Δ scheme gets affected at 0.27 p.u. and 0.8 p.u. load with 40 % and 60 % of voltage sag respectively.

Similarly, the 37.5 kW IM operating with Y- Δ scheme gets affected at 0.22 p.u. load on 60 percent voltage sag. Contrastingly, the delta connected IM does not get affected by same percentage of voltage sag, shown in Fig. 9. Overall, IM with Y- Δ scheme is more affected than the delta connected IM. Hence, the switchover point needs to be adjusted for a smooth operation. From the obtained test results, the new switchover point is determined and enforced in the controller.

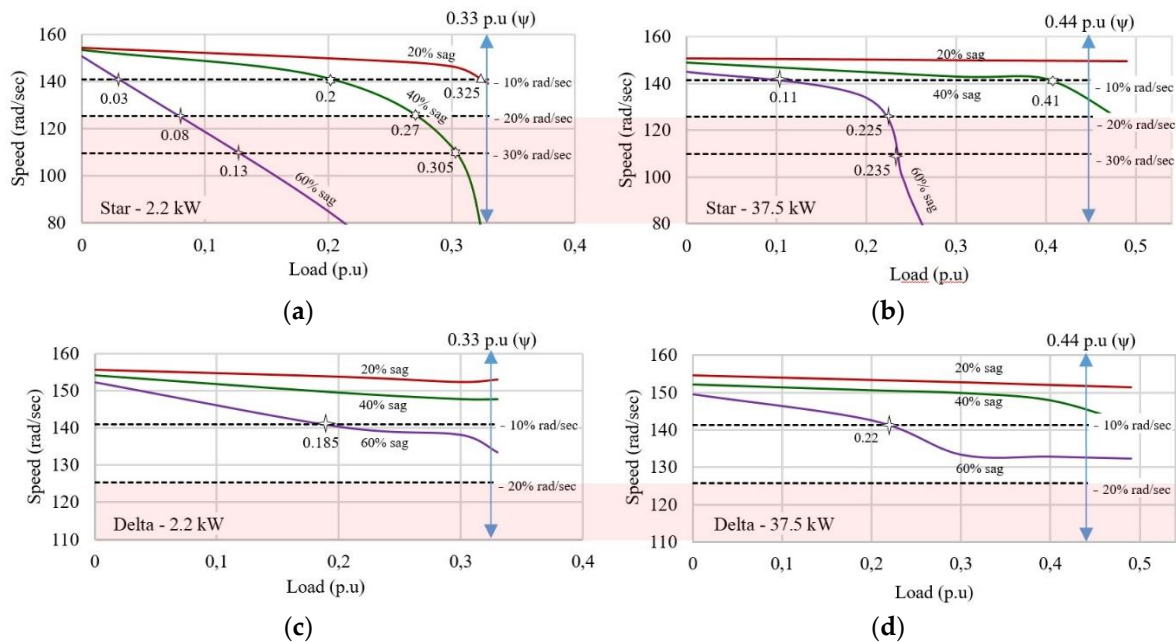


Figure 9. Speed variation of induction motors during voltage sag (20%, 40% and 60%): (a) Star connected 2.2 kW IM; (b) Delta connected 2.2 kW IM; (c) Star connected 37.5 kW IM; (d) Delta connected 37.5 kW IM.

4.2. Voltage Variation

An under voltage and over voltage is defined as the variation in rms voltage greater than 10 percent of its nominal value for longer than 1 min [24]. Under voltage fault is the main cause of overloaded circuits and poor voltage regulation that impacts on motor efficiency and lifespan. This under voltage in IM reduces the speed and overheats the windings which extend to insulation deterioration and winding failure. Also, the under-voltage fault lengthens the starting time of machine and raise the current flow in windings [27]. Similarly, overvoltage is the consequence of switching off large loads, tap changing of transformers and poor voltage regulation. Even though the occurrence of overvoltage is not frequent as under voltage, impacts of overvoltage on industrial motors are higher than the under-voltage fault [27]. Performance characteristics of lightly loaded 2.2 kW SCIM have been experimentally analyzed with 20 percent voltage variation on both star and delta connection individually, shown in Fig. 8 and using Matlab/Simulink software the 2.2 kW and 37.5 kW SCIM are analyzed.

The analyses have been performed at light loads (closer to the switch over point), because the aim of this paper is to analyze test machine under various electrical disturbances and modify the switch over point accordingly. The change in current and speed is the main consequence of voltage variation, hence, throughout the course of voltage variation, speed and current are monitored precisely.

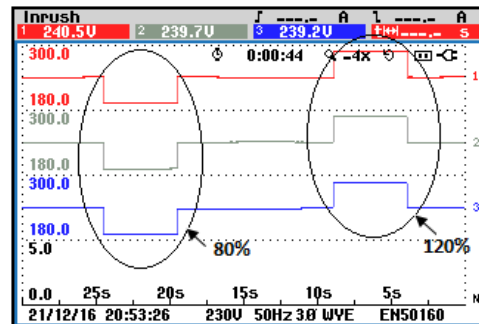


Figure 10. Voltage variation (80% and 120%).

During under voltage (20 %), the speed of star connected IM gets dropped to zero (halted) while trying to run beyond 0.32 p.u. load. Wherein delta connected IM is not affected with the same percentage of under voltage fault. Similarly, during over voltage, IM with Y- Δ scheme provides more beneficial effects such as, improvement in power factor and increase in energy conservation. Delta connected IM with over voltage create more thermal gradient that could even damage motor's stator windings. During voltage variation (under voltage or over voltage) on Y- Δ scheme based IM and normal (Δ) connected IM in the light load region, electromagnetic torque (T) and starting torque (T_{st}) of IM are obtained using the steady state torque equations (9) to (12) [28] and result are summarized in Table 3.

$$T = \frac{3}{\omega_s} \frac{U_{L-L}^2 \left(\frac{R_2^l}{s}\right)}{\left(\frac{R_2^l}{s}\right)^2 + (X_2^l)^2} \quad (9)$$

$$s = \frac{\omega_s - \omega_m}{\omega_s} \quad (10)$$

$$T \propto s U^2 \quad (11)$$

$$T_{st} = \frac{3}{\omega_s} \frac{U_{L-L}^2 R_2^l}{(R_1 + R_2^l)^2 + (X_1 + X_2^l)^2} \quad (12)$$

Where, U_{L-L} is the line to line voltage; s is the slip; ω_m is the motor speed and ω_s is the synchronous speed.

4.3. Voltage Unbalance

Voltage unbalance is one of the principal causes of power quality disturbances and it is evaluated in terms of voltage unbalance factor (VUF). The VUF is defined as the ratio of the negative sequence voltage (U_n) to the positive sequence voltage (U_p), usually expressed in percentage as in eqn. (13),(14) and (15) [24].

$$VUF (\%) = \frac{U_n}{U_p} \times 100 \quad (13)$$

$$U_p = \frac{1}{3}(U_a + \alpha U_b + \alpha^2 U_c) \quad (14)$$

$$U_n = \frac{1}{3}(U_a + \alpha^2 U_b + \alpha U_c) \quad (15)$$

where, $\alpha = e^{j120^\circ} = \cos 120^\circ + j\sin 120^\circ$, U_a, U_b, U_c are the phase voltage.

Effects of unbalanced voltages are equivalent to the superposition of negative-sequence voltage on the positive-sequence voltage. In the supply voltage, the positive sequence component is the direct function of the motor's efficiency and power factor. Similarly, negative sequence component influences negative sequence current flowing through motor windings that affects the motor torque and tends motor to draw higher current for equivalent mechanical load. Overall, voltage unbalance causes inefficiency and derating on induction motors and higher level of voltage unbalance can result in shaft vibration, failure of winding, failure of bearings, etc., [29]. To analyze machine's performance, induction motor in star and delta connection are operated with unbalance supply. In the laboratory, different value of voltage unbalance is generated using the AC programmable power supply, shown in Fig. 11. Negative sequence and positive sequence component are maintained same for both star and delta connected IM, mentioned in Table 3. The magnitude of voltage unbalance is computed using equation (13), (14) & (15), as well, measured using three phase power quality analyzer. Electrical and mechanical quantities are measured using power quality analyzer for estimating the efficiency and losses and thermal effect on IM is measured using thermal analyzer. Similarly, positive sequence torque (T_p), negative sequence torque (T_n) and net torque (T_{net}) are calculated using the steady state torque equation (16), (17) & (18) [28]. The results are tabularized in Table 3.

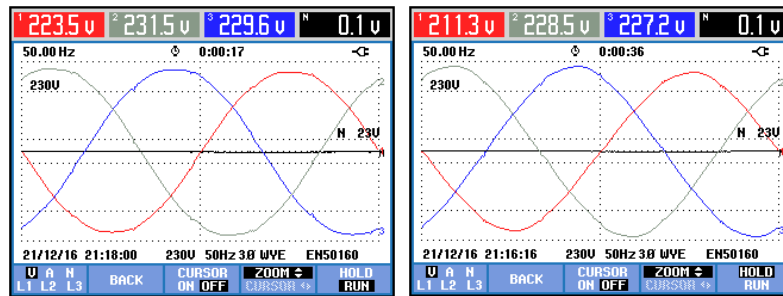


Figure 11. Voltage Unbalance (2.5% and 5%).

Investigating the effect of voltage unbalance results that, speed reduction is more in Y- Δ schemed IM than normal Δ connected IM. Similarly, Y- Δ schemed IM has experienced more shaft vibration and thermal gradient that indirectly entails the life span of machine. Overall, Y- Δ schemed IM are affected more than the delta connected IM during voltage unbalance.

$$T_{net} = T_p + T_n \quad (16)$$

$$T_p = \frac{3}{\omega_s} \frac{U_p^2(L-L) \left(\frac{R_2^l}{s}\right)}{\left(\frac{R_2^l}{s}\right)^2 + (X_2^l)^2} \quad (17)$$

$$T_n = \frac{3}{\omega_s} \frac{U_n^2(L-L) \left(\frac{R_2^l}{2-s}\right)}{\left(\frac{R_2^l}{2-s}\right)^2 + (X_2^l)^2} \quad (18)$$

4.4. Frequency Variation

Frequency variation is the deviance of fundamental frequency from its specified nominal value [32]. At any instant, the frequency of system depends on balance of load and generation. Frequency changes occur due to load switching, faults in transmission system, large block of deload or change in load, large generation going offline, control system tuning issues, etc., [31]. As the supply frequency is directly proportional to motor speed, frequency variation directly influences the speed of motor. For experimental analysis, a lightly loaded 2.2 kW SCIM with individual star and delta connection is energized using AC programmable power supply and for generalizing, two machines (2.2 kW and 37.5 kW) are analyzed using Matlab/Simulink software.

Similar to voltage analysis, frequency variation analysis on test motor is executed closer to switchover point. Speed and current fluctuation are the main consequences of frequency variation. During frequency variation, speed of Y- Δ schemed IM gets affected more than delta connected IM. Since the cooling effect of fan cooled induction motor (usually preferred in small and medium scale industries) is the direct function of rotational speed, the temperature gradient is more in star connected IM than the delta connected IM. Besides, Y- Δ scheme based IM draws less current with under frequency fault which results in loss reduction. On the whole, Y- Δ scheme based IM has less loss, but in energy conservation point of very less energy conservation is attained during under frequency. Likewise, during over frequency, the energy conservation and performance of star and delta connected IM has improved. From overall analysis, it is observed that, under frequency affects system more than the over frequency especially, the star connected IM. The percentage variation from the nominal values are summarized in Table 3.

4.5. Frequency Variation

The loss of one phase in three phase supply is termed as single phasing. An induction motor can suffer a single phasing failure due to any defects such as safety system breakdown, fuse broken, driver breaking, jumpers burning, substation failures, transmission transformer failures, etc., [30]. During single phasing fault, current flow increases on other two phases which creates voltage unbalance in larger magnitude that extends to winding damage [32]. Similarly, during single phasing, stationary machines fails to develop starting torque due to higher influence of negative sequence component in net torque development [33]. Considering this power quality problem, the 2.2 kW Y- Δ schemed IM is analyzed experimentally. Additionally, 2.2 kW and 37.5 kW Y- Δ scheme based IM are analyzed through Matlab/Simulink software for generalizing purpose. Single phasing fault is created experimentally using AC programmable power supply, during single phasing fault, magnitude of voltage unbalance is calculated using equation (13) and measured using three phase power quality analyzer.

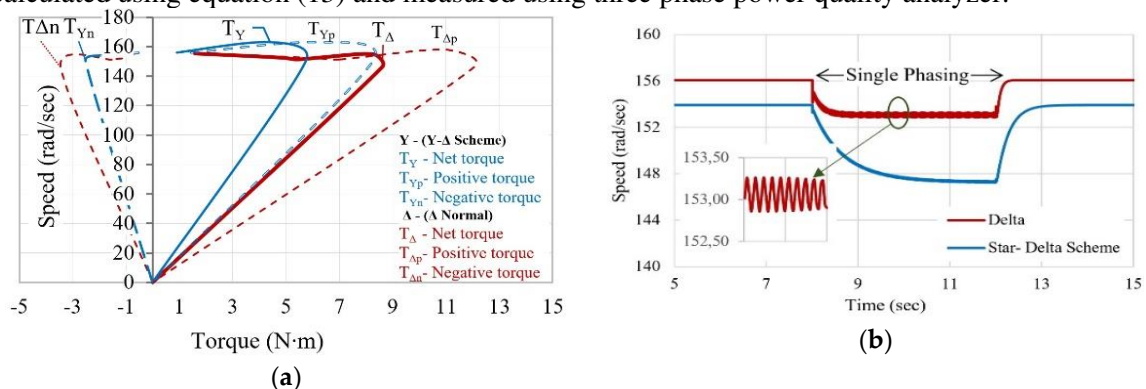


Figure 12. Speed and Torque variation during single phasing on 2.2 kW IM: (a) Speed-torque profile with single phasing; (b) Speed variation during single phasing at 0.2 p.u.

In addition to this, during single phasing, the positive sequence torque (T_p), negative sequence torque (T_n) and net torque (T_{net}) are computed using the steady state torque equations (16), (17) & (18) and plotted in Fig. 12a. From obtained result, it is realized that unbalance is created in large magnitude in Y- Δ schemed induction motor than the conventional delta connected induction motor. This consequence to high current flow in the stator windings resulting high thermal gradient. Also, it produces torque fluctuation and vibration in large magnitude. Long run of induction motor under single phasing fault could damage the bearing and other parts of the machine. During single phasing fault, speed droop and recovery time are higher in Y- Δ schemed induction motor as shown in Fig. 12b. Moreover, the test machine with Y- Δ scheme fails to drive the load above 0.3 p.u. load, but in delta connected induction motor stalling has not occurred. Also, the variation in the input and output parameters including temperature and vibration is higher than the nominal value in Y- Δ schemed test machine, whereas variation of quantities is in an acceptable limit up to 0.33 p.u. load in delta connected test machine. The percentage variation of input and output quantities from the nominal value during single phasing fault at light loads with star and delta connection are summarized in Table 3.

5. Summary of electrical perturbations

The influence of various electrical perturbations on induction motor under Y- Δ energy saving strategy is thoroughly investigated and compared to conventional delta connected IM. The results of investigations are as follows,

(i) Voltage Sag: Induction motor under Y- Δ energy saving strategy experiences speed drop in large magnitude, approximately three times larger than the conventional delta connected system, (Fig. 8). This creates an interruption in process, equipment damage and production losses. Also, sag malfunctions the protection system and even collapse the control system. Hence, this effect should be accounted and the switching point must be varied for continuous service.

(ii) Voltage Variation: Induction motor under Y- Δ energy saving strategy gets affected more than motor with delta connection. Drop in speed and rise in current are higher in case of Y- Δ scheme. The prolonged operation of the machine with under-voltage could interrupt the process and causes enormous loss of output.

Wherein, In the case of an over-voltage malfunction, the device has the advantages of energy conservation. Therefore, to attain uninterrupted operation during voltage variation the switchover point should be adjusted.

(iii) Voltage Unbalance: Y- Δ energy saving strategy experiences speed drop and more vibration affecting the process and causing enormous loss of production. As well as, fault increases the magnitude of line current and de-rates the machine. Therefore, adjusting the switching point for trouble-free service during voltage unbalance is mandatory.

(iv) Frequency Variation: As the motor speed is directly proportional to the input supply frequency, the motor speed is directly influenced by the frequency variation. During under-frequency fault, the line current of IM with Y- Δ scheme increased and there is no energy conservation during under-frequency fault. However, during over-frequency fault, the Y- Δ schemed IM conserves significant amount of energy. Therefore, the fitting of switching point in accordance to the frequency variation is essential.

(v) Single Phasing: The repercussion of single phasing fault in Y- Δ schemed IM is higher than other electrical perturbations. Motor fails to drive the load during single phasing failure and generates more losses for industries. Thus, the machine must be halted during single phasing failure instead of modifying the switchover point.

Table 3. Summary of various PQD on 2.2 kW and 37.5 kW induction motor in percentage variation.

| Voltage Variation | Operating Characteristics | Results for 2.2 kW IM at 0.32 p.u. load | | | | Results for 37.5 kW IM at 0.4 p.u. load | | | |
|--|---------------------------|---|---|---------------------|-----------------------|---|---|---------------------|------------|
| | | 80% (Under voltage) | | 120% (Over voltage) | | 80% (Under voltage) | | 120% (Over voltage) | |
| | | Y-Δ scheme | Normal (Δ) | Y-Δ scheme | Normal (Δ) | Y-Δ scheme | Normal (Δ) | Y-Δ scheme | Normal (Δ) |
| Speed | ↓ 7.9 | ↓ 0.13 | ↑ 4.16 | ↑ 0.81 | ↓ 0.74 | ↓ 0.33 | ↑ 0.40 | ↑ 0.133 | |
| Torque | ↑ 17.14 | ↓ 32.09 | ↓ 32.89 | ↓ 7.78 | ↑ 0.02 | ↓ 0.04 | ↓ 0.12 | ↓ 0.012 | |
| Current | ↑ 59.87 | ↓ 20.14 | ↓ 5.19 | ↑ 63.80 | ↑ 26.54 | ↓ 16.26 | ↓ 6.36 | ↑ 36.53 | |
| Power factor | ↓ 5.68 | ↑ 32.07 | ↓ 6.81 | ↓ 22.64 | ↓ 7.86 | ↑ 30.03 | ↓ 4.49 | ↓ 1.01 | |
| Starting torque | ↓ 39 | ↓ 37.33 | ↑ 44.08 | ↑ 47.22 | ↓ 34.85 | ↓ 35.96 | ↑ 44.13 | ↑ 39.22 | |
| Magnetic noise | Increases | No change | No change | Increased | -- | | | | |
| Voltage Unbalance | Operating Characteristics | Results for 2.2 kW SCIM | | | | | | | |
| | | 0.2 p.u. load | | | | 0.32 p.u. load | | | |
| | VUF | 2.5 % | | 5 % | | 2.5 % | | 5 % | |
| | Un (volts) / Up (volts) | 5.86 / 234.04 | | 11.73 / 232.85 | | 5.86 / 234.04 | | 11.73 / 232.85 | |
| | | Y- Δ Scheme | Normal (Δ) | Y- Δ Scheme | Normal (Δ) | Y- Δ Scheme | Normal (Δ) | Y- Δ Scheme | Normal (Δ) |
| | Speed | ↓ 0.55 | ↓ 0.34 | ↓ 0.96 | ↓ 0.61 | ↓ 0.86 | ↓ 0.34 | ↓ 1.44 | ↓ 0.82 |
| | Torque | ↑ 33.03 | ↑ 20.32 | ↑ 38.72 | ↑ 35.24 | ↑ 15.36 | ↑ 27.4 | ↑ 26.94 | ↑ 38.33 |
| | Power factor | ↓ 0.41 | ↓ 3.59 | ↓ 2.41 | ↓ 2.12 | ↑ 1.04 | ↓ 0.62 | ↑ 0.23 | ↓ 2.68 |
| | Temperature | ↑ 0.16 | ↑ 0.69 | ↑ 10.42 | ↑ 1.00 | ↑ 3.10 | ↑ 0.69 | ↑ 7.84 | ↑ 3.56 |
| | Voltage Unbalance | Operating Characteristics | Results for 37.5 kW SCIM | | | | | | |
| 0.2 p.u. load | | | | 0.4 p.u. load | | | | | |
| VUF | | 2.5 % | | 5 % | | 2.5 % | | 5 % | |
| Un (volts) / Up (volts) | | 5.597 / 224.4 | | 11.62 / 219.8 | | 5.597 / 224.4 | | 11.62 / 219.8 | |
| | | Y- Δ Scheme | Normal (Δ) | Y- Δ Scheme | Normal (Δ) | Y- Δ Scheme | Normal (Δ) | Y- Δ Scheme | Normal (Δ) |
| Speed | | ↓ 0.13 | ↓ 0.11 | ↓ 0.25 | ↓ 0.20 | ↓ 0.22 | ↓ 0.18 | ↓ 0.54 | ↓ 0.40 |
| Torque | | ↑ 2.58 | ↑ 25.8 | ↑ 11.48 | ↑ 84.28 | ↑ 2 | ↑ 7.37 | ↑ 3.04 | ↑ 28.37 |
| Power factor | | ↓ 4.25 | ↓ 18.36 | ↓ 14.89 | ↓ 16.97 | ↑ 2.32 | ↓ 8.16 | ↑ 4.65 | ↓ 38.77 |
| Temperature | | -- | | | | | | | |
| Frequency Variation | | Operating Characteristics | Results for 2.2 kW IM at 0.32 p.u. load | | | | Results for 37.5 kW IM at 0.4 p.u. load | | |
| | 95% (Under Frequency) | | 105% (Over Frequency) | | 95% (Under Frequency) | | 105% (Over Frequency) | | |
| | Y- Δ Scheme | | Normal (Δ) | Y- Δ Scheme | Normal (Δ) | Y- Δ Scheme | Normal (Δ) | Y- Δ Scheme | Normal (Δ) |
| | Speed | ↓ 5.44 | ↓ 5.31 | ↑ 7.61 | ↑ 6.40 | ↓ 4.95 | ↓ 4.92 | ↑ 5.02 | ↑ 4.99 |
| | Torque | ↓ 2.71 | ↓ 18.74 | ↓ 23.34 | ↓ 18.95 | ↓ 0.257 | ↓ 0.281 | ↓ 0.171 | ↓ 0.244 |
| | Current | ↑ 10.35 | ↑ 20.22 | ↑ 10.34 | ↓ 4.58 | ↑ 5.52 | ↑ 10.81 | ↑ 5.55 | ↓ 12.01 |
| | Power factor | ↓ 0.61 | ↓ 9.29 | ↓ 0.44 | ↑ 12.84 | ↓ 2.24 | ↓ 1.01 | ↓ 1.12 | ↑ 1.01 |
| Starting torque | ↑ 7.26 | ↑ 11.07 | ↓ 4.86 | ↓ 1.82 | ↑ 10.80 | ↑ 12.81 | ↓ 9.17 | ↓ 10.67 | |
| Slip | ↓ 6.52 | ↓ 26.86 | ↓ 19.63 | ↓ 17.45 | ↓ 6.43 | ↓ 12.28 | ↓ 0.52 | ↓ 4.76 | |
| Single phasing | Operating Characteristics | Results for 2.2 kW IM | | | | Results for 37.5 kW IM | | | |
| | | 0.2 p.u. load | | 0.32 p.u. load | | 0.3 p.u. load | | 0.4 p.u. load | |
| | | Y-Δ Scheme | Normal (Δ) | Y-Δ Scheme | Normal (Δ) | Y-Δ Scheme | Normal (Δ) | Y-Δ Scheme | Normal (Δ) |
| | Speed | ↓ 2.45 | ↓ 0.95 | Stall | ↓ 0.95 | ↓ 1.20 | ↓ 0.40 | Stall | ↓ 0.73 |
| | Torque | ↑ 187.57 | ↑ 26.41 | Stall | ↑ 13.39 | ↑ 133.1 | ↑ 89.0 | Stall | ↑ 57.4 |
| Avg. line current | ↑ 135.96 | ↑ 68.67 | ↑ 293.9 | ↑ 75.37 | ↑ 159.2 | ↑ 144.4 | ↑ 316.19 | ↑ 162.92 | |
| Temperature °F | ↑ 17.68 | ↑ 17.68 | Stall | Stall | -- | | | | |
| All the above results are in percentage | | | | | | | | | |
| ↑ represents increase from its nominal value | | | | | | | | | |
| ↓ represents decrease from its nominal value | | | | | | | | | |

Overall performance of induction motor (2.2 kW and 37.5 kW) under Y- Δ energy conservation scheme and induction motor with normal Δ connection is analyzed under the influence of various power quality disturbances. Consequence of the analysis is tabularized with percentage variation from nominal value in Table 3.

Hence, by considering all these power quality effects in the existing Y- Δ energy conservation scheme an option for readjusting switchover point (ψ) is provided in the proposed control strategy. In view of Fig. 2a and [8], the 2.2 kW IM in star mode can be operated up to 0.33 p.u., but on consideration of various power quality disturbances, IM cannot be operated up to 0.33 p.u. load. Similarly, 37.5 kW IM cannot be operated up to 0.44 p.u. load during PQD. Therefore, a new strategy is developed in controller to provide uninterrupted operation by readjusting the switchover point (ψ), discussed in subsequent subsection. Percentage variation in energy conservation under various PQD from nominal value and change in switchover point (ψ) corresponding to the PQD are presented in Table 4.

Table 4. Percentage variation in energy conservation under various PQD.

| PQD | Results for 2.2 kW IM | | Results for 37.5 kW IM | |
|----------------------|------------------------------|-------------|------------------------------|-------------|
| | Switch over point (Ψ) | % Variation | Switch over point (Ψ) | % Variation |
| Nominal | 0.33 | -- | 0.44 | -- |
| Under voltage (20%) | 0.25 | ↓ 74.89 | 0.24 | ↓ 64.74 |
| Over voltage (20%) | 0.61 | ↑ 140.3 | 0.64 | ↑ 108.5 |
| Under frequency (5%) | 0.12 | ↓ 10.6 | 0.08 | No EC |
| Over frequency (5%) | 0.58 | ↑ 3.475 | 0.85 | ↑ 40.38 |
| Unbalance (5%) | 0.32 | ↓ 46.93 | 0.39 | ↓ 77.4 |
| Single phasing | 0.16 | ↓ 14.33 | 0.19 | No EC |

All the above results are in percentage
 ↑ represents increase from its nominal value
 ↓ represents decrease from its nominal value

6. Intelligent Switching Mechanism Intelligent Switching Mechanism

In addition to existing energy conservation scheme discussed in [5], control strategy is embedded with safe restarting and switchover point readjustment feature. This feature facilitates to continue the process without any interruption and to increase the lifespan of machine.

6.1. Safe restarting

From the investigation of the EC system based on a Y- Δ scheme, if the Y- Δ scheme enabled machine is deliberately disturbed by any grid disruptions or by an operator accidentally, it starts again in star contact only. Nevertheless, the star-connected induction motor does not resume at high loads due to low starting torque (about one-third of the based delta motor). Starting the IM with a star contact often increases the start time, leads to thermal stress and lifespan reduction. Therefore, during the process, the IM must resume in the star contact or delta contact by considering the recess load point from past interruption. Hence, the previous operating mode (Y and Δ) storage facility is installed in the microcontroller to resume the motor in star or delta connection. This function is mandatory for the Y- Δ scheme enabled machine to establish the required starting torque. For example, induction motor is interrupted while running at 60 percent of its full load, star-connected machine fails to resume due to insufficient starting torque shown in Fig. 13 with stripped lines, but the machine with delta connection resumes in 23 millisecond shown in a continuous line.

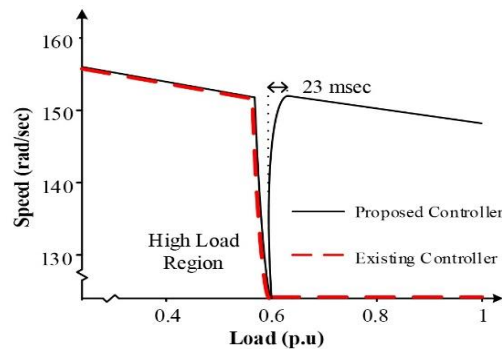


Figure 13. Speed profile of test machine at 0.6 p.u. load during restart.

6.2. *Switchover point readjustment*

The motor loses its stability during various electrical disturbances and causes loss of production. From the analysis of various power quality issues in Y-Δ based energy conservation scheme, readjustment of switchover point (ψ) is mandatory for obtaining more energy conservation as well as to provide uninterrupted service. Therefore, the preconfigured value of the switchover point will be changed automatically based on recurring electrical disruptions. Automatic readjustment of switchover point is depending upon the quality of power received in industry and it can be readjusted externally by considering the power quality impact on process and end product. Therefore, it is possible to conserve more energy without interrupting the process using the proposed control strategy shown in Fig.14.

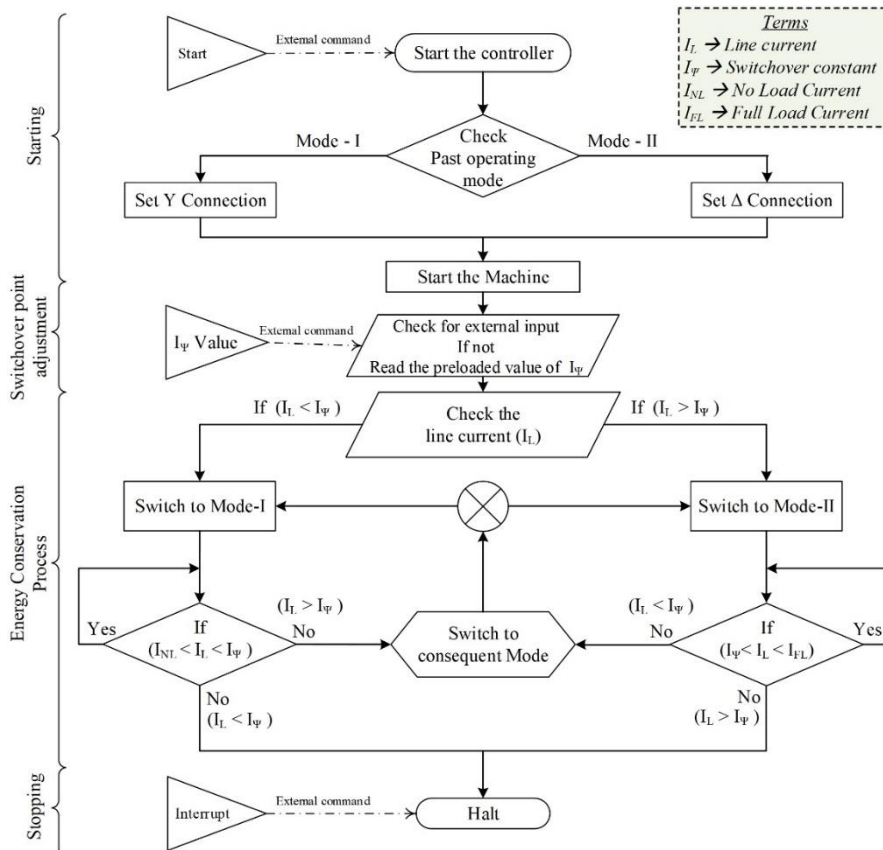


Figure 14. Proposed Intelligent Switching Mechanism for induction motor.

7. Conclusion

Economic energy conservation is an important scenario for any industry, but reliability of preferred energy conservation method is also very important. Hence, the performance of an IM under Y- Δ EC scheme is evaluated and outlined in this paper with the effects of different energy value disruptions. The analyzed results convey that the effects of electrical perturbation cause serious problems in production with an increase in operating costs, motor losses and motor failure. Considering these effects on induction motor, an optimal energy saving strategy is developed with memory storage and switchover point readjustment features, in which, the switchover adjustment may depend upon the quality of power received in the industry and the sensitivity of the end product. Therefore, no matter how much resources are used to conserve energy, proactivity analyzing and responding to anticipation risk is extremely important.

References

1. N. Kumar, T. R. Chelliah and S. P. Srivastava, "Energy conservation study on induction motors using MATLAB/Simulink for enhancing electric machinery courses," Proceedings of IEEE International Conference on Teaching, Assessment, and Learning for Engineering (TALE) 2012, Hong Kong, 2012, pp. H4B-10-H4B-16, doi: 10.1109/TALE.2012.6360358.
2. Gnacinski, P. Energy saving work of frequency controlled induction cage machine. *Energy Conversion and Management*, **2007**; 48, 919–26. DOI:10.1016/j.enconman.2006.08.002.
3. Kothals-Altes, W. Motor winding; U.S. Patent 1 267 232, May 21, 1918.
4. Jannati, M.; et. al, A review on Variable Speed Control techniques for efficient control of Single-Phase Induction Motors: Evolution, classification, comparison. *Renewable and Sustainable Energy Reviews*, Available online 16 November 2016, ISSN 1364-0321.
5. Alger, P.L.; Hughes, A. New 3-phase winding of low m.m.f. harmonic content. *Proceedings of the Institution of Electrical Engineers*, **1971**, 118, 607-608. DOI: 10.1049/piee.1970.0293
6. Taylor, N.R.; Taylor, P.A. Automatic load seeking control for a motor; U.S. Patent 4 413 218, Nov. 1, 1983.
7. Gjota, R. Winding arrangement of a stator and/or rotor of a three-phase generator or electromotor with improved performances. U.S. Patent 4 710 661, Dec. 1, **1987**.
8. Ferreira, F.J.T.E.; De Almeida, T. Method for in-field evaluation of the stator winding connection of three-phase induction motors to maximize efficiency and power factor. *IEEE Transactions on Energy Conversion* **2006**, 21, 370–379. DOI: 10.1109/TEC.2006.874248.
9. Kostic, M.M.; Radakovic, J. Induction Motors with YY / Δ Connection Change for Efficiency and Power Factor Increasing at Partial Loads. *Journal of Electrical Engineering*, **2006**, 19, 85–98.
10. Blinov, A.; Vinnikov, D.; Jalakas, T. Loss calculation methods of half-bridge square-wave inverters. *Electronics and Electrical Engineering*, **2011**; 7, 9–14. doi:10.5755/j01.eee.113.7.604.
11. Marouani, K.; Khaldi, M.; Khoucha, F.; Kheloui, A. Switching losses and harmonic currents evaluation of PWM techniques for VSI-fed dual stator induction motor drive. *2009 17th Mediterranean Conference on Control and Automation*, Thessaloniki, **2009**, pp. 1492-1497.
12. Sakthivel, V.P.; Subramanian, S. On-site efficiency evaluation of three-phase induction motor based on particle swarm optimization. *Energy*, **2011**, 36 (3), 1713-1720, ISSN 0360-5442.
13. Lu, B.; Habetler, T.G.; Harley, R.G. A survey of efficiency-estimation methods for in-service induction motors. *IEEE Trans Ind Appl*, **2006**, 42 (4), pp. 924–933.
14. Sivarani, T.S. Jawhar J.S., Cumar, A.K. Intensive random carrier pulse width modulation for induction motor drives based on hopping between discrete carrier frequencies. *IET Power Electron.*, **2016**, 9, pp. 1–10.

15. Singh, R.R.; Thanga Raj, C. Enforcement of cost-effective energy conservation on single-fed asynchronous machine using a novel switching strategy, *Energy* **2017**, 126, pp. 179-191, <https://doi.org/10.1016/j.energy.2017.03.003>.
16. Mohan, H.; Singh, R.R.; Agrawal, K.; Kumar, B.A.; Thanga Raj, C. Energy conservation on induction motors drives with immune control strategy using full spectrum simulator, *2017 International Conference on Computer Communication and Informatics (ICCCI)*, Coimbatore, **2017**, pp. 1-6. doi: 10.1109/ICCCI.2017.8117800
17. Woronowicz, K.; Palka, R. Optimized thrust control of linear induction motors by a compensation approach. *International Journal of Applied Electromagnetics and Mechanics* **2004**, 19(1-4), pp. 533-536.
18. Wardach, M.; Bonislawski, M; Palka, R.; Paplicki, P.; Prajzendanc, P. Hybrid Excited Synchronous Machine with Wireless Supply Control System. *Energies* **2019**, 12, 3153, doi:10.3390/en12163153.
19. Paplicki, P.; Wardach, M.; Bonislawski, M.; Palka, R. Simulation and experimental results of hybrid electric machine with a novel flux control strategy. *Arch. Electr. Eng.* **2015**, 64, 37–51.
20. Christopoulos, G.A.; Zafiris, A.; Safacas, A.N. Energy savings and operation improvement of rotating cement kiln by the implementation of a unique new drive system. *IET Electr. Power Appl.*, **2016**, 10 (2), pp. 101–109.
21. IEEE Standard Test Procedure for Polyphase Induction Motors and Generators. IEEE Standard 112TM-2004, 2004; 1-109. DOI: 10.1109/IEEESTD.1991.114383.
22. EIA report. Average Price of Electricity to Ultimate Customers by End-Use Sector. October 2015 and 2014 (Cents per Kilowatt-hour) electric power monthly data for October 2015. Release date: December 24, 2015.
23. Manish Kumar Saini, Rajiv Kapoor. Classification of power quality events – A review. *International Journal of Electrical Power & Energy Systems* **2012**; 43: 11-19. DOI:10.1016/j.ijepes.2012.04.045
24. IEEE Recommended Practice for Monitoring Electric Power Quality. IEEE Standard 1159TM-2009, 2009; 1-76. DOI: 10.1109/IEEESTD.1995.79050
25. Rolán, A.; Córcoles, F.; Pedra, J.; Monjo, L.; Bogarra, S. Testing of three-phase equipment under voltage sags. *IET Electr. Power Appl.*, **2015**, 9 (4), pp. 287–296.
26. Milanovic, J.V.; Aung, M.T.; Vegunta S.C. The Influence of Induction Motors on Voltage Sag Propagation — Part I: Accounting for the Change in Sag Characteristics. *IEEE Transactions on Power Delivery*, **2008**, 23, 1063–1071. DOI: 10.1109/TPWRD.2007.915846
27. Wallace, A.; Von Jouanne, A.; Wiedenbrug, E.; Ünsal, A.; Andrews, P. The Effects of Nonideal Voltage and Winding Conditions on the Performance of Induction Motors. *Electr. Power Components Syst.*, 2001, 29, 543–554. DOI:10.1080/153250001300338772.
28. Dubey, G.K., Fundamentals of electrical drives. **2002**, CRC press.
29. Reineri, C.A.; Gómez, J.C.; Balaguer, E.B.; Morcos, M.M. Experimental Study of Induction Motor Performance with Unbalanced Supply. *Electr. Power Components Syst.*, **2006**, 34, 817–829. DOI:10.1080/15325000500488636.
30. NEMA Standards Information Guide for General Purpose Industrial AC Small and Medium Squirrel-Cage Induction Motor Standards. NEMA Standards Publication Condensed MG 1-2007.
31. Bonnett, A.H. The impact that voltage and frequency variations have on AC induction motor performance and life in accordance with NEMA MG-1 standards. *Pulp and Paper Industry Conference* (Cat. No.99CH36338), **1999**. DOI: 10.1109/PAPCON.1999.779341.
32. Agamlloh, E.B.; Peele, S.; Grappe, J. Induction Motor Single-Phasing Performance Under Distribution Feeder Recloser Operations. *IEEE Transactions on Industry Applications*, **2014**, 50 (2), pp. 1568-1576. DOI:10.1109/TIA.2013.2279188

33. Kersting, W.H. Causes and Effects of Single-Phasing Induction Motors. *IEEE Transactions on Industry Applications*, **2005**, 41, 1499–1505. DOI: 10.1109/TIA.2005.857467.